

The TAIGA experiment

M. Tluczykont

*Institut für Experimentalphysik, Universität Hamburg, Hamburg, D-22 761 Germany
martin.tluczykont@physik.uni-hamburg.de*

I.I. Astapov

National Research Nuclear University MPhI, Moscow, 115409 Russia

A.K. Awad

Institut für Experimentalphysik, Universität Hamburg, Hamburg, D-22 761 Germany

P.A. Bezyazeev

Research Institute of Applied Physics, Irkutsk State University, Irkutsk, 664003 Russia

M. Blank

Institut für Experimentalphysik, Universität Hamburg, Hamburg, D-22 761 Germany

E.A. Bonvech

Skobeltsyn Institute of Nuclear Physics, Moscow State University, Moscow, 119991 Russia

A.N. Borodin

Joint Institute for Nuclear Research, Dubna, Moscow oblast, 141980 Russia

A.V. Bulan

Skobeltsyn Institute of Nuclear Physics, Moscow State University, Moscow, 119991 Russia

M. Brückner

Deutsches Elektronen-Synchrotron DESY, Zeuthen, 15738 Germany

N.M. Budnev

Research Institute of Applied Physics, Irkutsk State University, Irkutsk, 664003 Russia

A. Chiavassa

*Physics Department of the University of Torino and Istituto Nazionale di Fisica Nucleare,
Torino, 10125 Italy*

D.V. Chernov

Skobeltsyn Institute of Nuclear Physics, Moscow State University, Moscow, 119991 Russia

A.N. Dyachok

Research Institute of Applied Physics, Irkutsk State University, Irkutsk, 664003 Russia

A.R. Gafarov

Research Institute of Applied Physics, Irkutsk State University, Irkutsk, 664003 Russia

A.Yu. Garmash

Novosibirsk State University, Novosibirsk, 630090 Russia

*Budker Institute of Nuclear Physics, Siberian Branch, Russian Academy of Sciences,
Novosibirsk, 630090 Russia*

V.M. Grebenyuk

Joint Institute for Nuclear Research, Dubna, Moscow oblast, 141980 Russia

Dubna University, Dubna, Moscow oblast, 141980 Russia

O.A. Gress

Research Institute of Applied Physics, Irkutsk State University, Irkutsk, 664003 Russia

E. Gress

Research Institute of Applied Physics, Irkutsk State University, Irkutsk, 664003 Russia

T.I. Gress

Research Institute of Applied Physics, Irkutsk State University, Irkutsk, 664003 Russia

O.G. Grishin

Research Institute of Applied Physics, Irkutsk State University, Irkutsk, 664003 Russia

A.A. Grinyuk

Joint Institute for Nuclear Research, Dubna, Moscow oblast, 141980 Russia

D. Horns

Institut für Experimentalphysik, Universität Hamburg, Hamburg, D-22 761 Germany

A.L. Ivanova

Novosibirsk State University, Novosibirsk, 630090 Russia

Research Institute of Applied Physics, Irkutsk State University, Irkutsk, 664003 Russia

N.N. Kalmykov

Skobel'syn Institute of Nuclear Physics, Moscow State University, Moscow, 119991 Russia

V.V. Kindin

National Research Nuclear University MEPhI, Moscow, 115409 Russia

S.N. Kiryuhin

Research Institute of Applied Physics, Irkutsk State University, Irkutsk, 664003 Russia

R.P. Kokoulin

National Research Nuclear University MEPhI, Moscow, 115409 Russia

K.G. Kompaniets

National Research Nuclear University MEPhI, Moscow, 115409 Russia

E.E. Korosteleva

Skobeltsyn Institute of Nuclear Physics, Moscow State University, Moscow, 119991 Russia

V.A. Kozhin

Skobeltsyn Institute of Nuclear Physics, Moscow State University, Moscow, 119991 Russia

E.A. Kravchenko

Novosibirsk State University, Novosibirsk, 630090 Russia

*Budker Institute of Nuclear Physics, Siberian Branch, Russian Academy of Sciences,
Novosibirsk, 630090 Russia*

A.P. Kryukov

Skobeltsyn Institute of Nuclear Physics, Moscow State University, Moscow, 119991 Russia

L.A. Kuzmichev

Skobeltsyn Institute of Nuclear Physics, Moscow State University, Moscow, 119991 Russia

A.A. Lagutin

Altai State University, Barnaul, Altai krai, 656049 Russia

M. Lavrova

Joint Institute for Nuclear Research, Dubna, Moscow oblast, 141980 Russia

E. Lemeshev

Research Institute of Applied Physics, Irkutsk State University, Irkutsk, 664003 Russia

B.K. Lubsandorzhev

Institute for Nuclear Research, Russian Academy of Sciences, Moscow, 117312 Russia

N.B. Lubsandorzhev

Skobeltsyn Institute of Nuclear Physics, Moscow State University, Moscow, 119991 Russia

A.D. Lukanov

Institute for Nuclear Research, Russian Academy of Sciences, Moscow, 117312 Russia

D.S. Lukyantsev

Research Institute of Applied Physics, Irkutsk State University, Irkutsk, 664003 Russia

R.R. Mirgazov

Research Institute of Applied Physics, Irkutsk State University, Irkutsk, 664003 Russia

R. Mirzoyan

Max Planck Institute for Physics, Munich, 80805 Germany

Research Institute of Applied Physics, Irkutsk State University, Irkutsk, 664003 Russia

R.D. Monkhoev

Research Institute of Applied Physics, Irkutsk State University, Irkutsk, 664003 Russia

E.A. Osipova

Skobeltsyn Institute of Nuclear Physics, Moscow State University, Moscow, 119991 Russia

A.L. Pakhorukov

Research Institute of Applied Physics, Irkutsk State University, Irkutsk, 664003 Russia

A. Pan

Joint Institute for Nuclear Research, Dubna, Moscow oblast, 141980 Russia

L.V. Pankov

Research Institute of Applied Physics, Irkutsk State University, Irkutsk, 664003 Russia

A.D. Panov

Skobeltsyn Institute of Nuclear Physics, Moscow State University, Moscow, 119991 Russia

A.A. Petrukhin

National Research Nuclear University MEPhI, Moscow, 115409 Russia

D.A. Podgrudkov

Skobeltsyn Institute of Nuclear Physics, Moscow State University, Moscow, 119991 Russia

V.A. Poleschuk

Research Institute of Applied Physics, Irkutsk State University, Irkutsk, 664003 Russia

E.G. Popova

Skobeltsyn Institute of Nuclear Physics, Moscow State University, Moscow, 119991 Russia

A. Porelli

Deutsches Elektronen-Synchrotron DESY, Zeuthen, 15738 Germany

E.B. Postnikov

Skobeltsyn Institute of Nuclear Physics, Moscow State University, Moscow, 119991 Russia

V.V. Prosin

Skobeltsyn Institute of Nuclear Physics, Moscow State University, Moscow, 119991 Russia

V.S. Ptuskin

Pushkov Institute of Terrestrial Magnetism, Ionosphere and Radio Wave Propagation, Russian Academy of Sciences, Troitsk, Moscow, 142190 Russia

A.A. Pushnin

Research Institute of Applied Physics, Irkutsk State University, Irkutsk, 664003 Russia

R.I. Raikin

Altai State University, Barnaul, Altai krai, 656049 Russia

A.Y. Razumov

Skobeltsyn Institute of Nuclear Physics, Moscow State University, Moscow, 119991 Russia

G.I. Rubtsov

Institute for Nuclear Research, Russian Academy of Sciences, Moscow, 117312 Russia

E.V. Ryabov

Research Institute of Applied Physics, Irkutsk State University, Irkutsk, 664003 Russia

Y.I. Sagan

Joint Institute for Nuclear Research, Dubna, Moscow oblast, 141980 Russia

Dubna University, Dubna, Moscow oblast, 141980 Russia

V.S. Samoliga

Research Institute of Applied Physics, Irkutsk State University, Irkutsk, 664003 Russia

I. Satyshev

Joint Institute for Nuclear Research, Dubna, Moscow oblast, 141980 Russia

Yu.A. Semeny

Research Institute of Applied Physics, Irkutsk State University, Irkutsk, 664003 Russia

A.A. Silaev

Skobeltsyn Institute of Nuclear Physics, Moscow State University, Moscow, 119991 Russia

A.A. Silaev(junior)

Skobeltsyn Institute of Nuclear Physics, Moscow State University, Moscow, 119991 Russia

A.Yu. Sidorenkov

Institute for Nuclear Research, Russian Academy of Sciences, Moscow, 117312 Russia

A.V. Skurikhin

Skobeltsyn Institute of Nuclear Physics, Moscow State University, Moscow, 119991 Russia

A.V. Sokolov

Novosibirsk State University, Novosibirsk, 630090 Russia

*Budker Institute of Nuclear Physics, Siberian Branch, Russian Academy of Sciences,
Novosibirsk, 630090 Russia*

Y. Suvorkin

Research Institute of Applied Physics, Irkutsk State University, Irkutsk, 664003 Russia

L.G. Sveshnikova

Skobeltsyn Institute of Nuclear Physics, Moscow State University, Moscow, 119991 Russia

V.A. Tabolenko

Research Institute of Applied Physics, Irkutsk State University, Irkutsk, 664003 Russia

A.B. Tanaev

Research Institute of Applied Physics, Irkutsk State University, Irkutsk, 664003 Russia

B.A. Tarashansky

Research Institute of Applied Physics, Irkutsk State University, Irkutsk, 664003 Russia

M. Ternovoy

Research Institute of Applied Physics, Irkutsk State University, Irkutsk, 664003 Russia

L.G. Tkachev

Joint Institute for Nuclear Research, Dubna, Moscow oblast, 141980 Russia

Dubna University, Dubna, Moscow oblast, 141980 Russia

N. Ushakov

Institute for Nuclear Research, Russian Academy of Sciences, Moscow, 117312 Russia

A. Vaidyanathan

Novosibirsk State University, Novosibirsk, 630090 Russia

P.A. Volchugov

Skobeltsyn Institute of Nuclear Physics, Moscow State University, Moscow, 119991 Russia

N.V. Volkov

Altai State University, Barnaul, Altai krai, 656049 Russia

D. Voronin

Institute for Nuclear Research, Russian Academy of Sciences, Moscow, 117312 Russia

R. Wischnewski

Deutsches Elektronen-Synchrotron DESY, Zeuthen, 15738 Germany

I.I. Yashin

National Research Nuclear University MEPhI, Moscow, 115409 Russia

A.V. Zagorodnikov

Research Institute of Applied Physics, Irkutsk State University, Irkutsk, 664003 Russia

D.P. Zhurov

Research Institute of Applied Physics, Irkutsk State University, Irkutsk, 664003 Russia

Irkutsk National Research Technical University, Irkutsk, Russia

The Tunka Advanced Instrument for Gamma-ray and cosmic ray Astrophysics (TAIGA) is a hybrid experiment for the measurement of Extensive Air Showers (EAS) with good spectral resolution in the TeV to PeV energy range. In this domain, the long-sought Pevatrons can be detected. Currently the hybrid TAIGA detector combines two wide angle shower front Cherenkov light sampling timing arrays (HiSCORE and Tunka-133), two 4m class, 10° aperture Imaging Air Cherenkov Telescopes (IACTs) and 240 m² surface and underground charged particle detector stations. Our goal is to introduce a new hybrid reconstruction technique, combining the good angular and shower core resolution of HiSCORE with the gamma-hadron separation power of imaging telescopes. This approach allows to maximize the effective area and simultaneously to reach a good gamma-hadron separation at low energies (few TeV). At higher energies, muon detectors are planned to enhance gamma-hadron separation. During the commissioning phase of the first and second IACT, several sources were observed. First detections of known sources with the first telescope show the functionality of the TAIGA IACTs. Here, the status of the TAIGA experiment will be presented, along with first results from the current configuration.

Keywords: Gamma-rays: experiments; Observations: Crab Nebula.

1. Introduction

TAIGA stands for Tunka Advanced Instrument for Gamma-ray and cosmic ray Astrophysics, and is a hybrid instrument designed to access the gamma-ray energy range from approx. 1 TeV to several 100s of TeV. The experiment is located at an altitude of 675m above sea level on the site of the Tunka-133¹ cosmic ray array ($51^\circ 48' 35''$ N, $103^\circ 04' 02''$ E). Observations in this energy range are motivated by several questions of Astroparticle and particle physics. The presence of cosmic ray (CR) accelerators within our Galaxy can be inferred from observations of diffuse and extended gamma-ray emission in the High-Energy (HE)² and Very-High-Energy (VHE) range³⁻⁵ e.g. These Gamma-ray emissions result from the decay of neutral

pions, which are produced in interactions of the accelerated cosmic rays with the ambient interstellar medium, i.e. molecular gas clouds, which effectively act as CR tracers.⁶ The gamma-ray energy range from 10 TeV to few 100 TeV is crucial for the search for the Galactic Pevatrons, which accelerate cosmic ray particles up to knee-energies (approx. 3 PeV proton energy). Due to the typical inelasticity of hadronic interactions, the cutoff energy of Pevatrons in the gamma-ray regime is located at energies of several 100 TeV. Hard gamma-ray spectra in this energy range are much less ambiguously attributable to the hadronic rather than leptonic emission mechanism, because the cross-section for inverse Compton scattering drops with increasing energy (Klein-Nishina regime). Recent neutrino observations⁷ and the detection of gamma-rays at ultra high energies by LHAASO⁸ emphasize the potential of the search for the Galactic Pevatrons. The detection of Pevatrons, and their spectroscopic, and morphological resolution in their cutoff energy regime are the main physics goals of TAIGA.

Beyond 10^{17} eV, the origin of CR is assumed to be extra-Galactic (EG). Due to the development of intergalactic pair cascades, the accelerators of EG cosmic rays (EGCR) might exhibit a halo-like gamma-ray emission. Furthermore, one can expect an enhancement of EGCR from the local galactic supercluster.⁹ The intergalactic pair cascades from that direction could create an anisotropic gamma-ray emission, observable with a wide field of view.

In the energy range of 100 TeV to several PeV, absorption due to pair creation becomes relevant also for Galactic sources. The attenuation of Galactic gamma-ray signals via production of e^+e^- -pairs reaches a maximum around 100 TeV from the Galactic interstellar radiation field (IRF) and at 2 PeV from the cosmic microwave background (CMB).¹⁰ This opens up the possibility to measure the density of the IRF, provided the distance of the emitting object is known. At PeV energies, the relevant field is the CMB, which is universal and very well known. Therefore, a possibility might exist to measure distances from a CMB absorption feature, i.e. cutoff in energy spectra of the most energetic Galactic gamma-ray sources. Another variable comes into play when considering the possibility of photon/axion conversion¹¹ or photon/hidden-photon oscillations,¹² because axions and hidden-photons could propagate without interaction, reconvert to photons, thus reducing the attenuation effect by pair production. Another fundamental effect on the attenuation by pair production might be the modification of the e^+e^- pair production threshold due to Lorentz Invariance violation. In a more direct way, other, non-thermal, dark matter candidates (e.g. wimpzillas) with masses ranging from 10^{12} GeV to 10^{16} GeV can be searched for in the energy range considered.

Furthermore, the chemical composition of Cosmic rays can be measured with TAIGA in the transition range from a Galactic to extragalactic origin ($\approx 10^{15}$ eV to 10^{17} eV) and in the energy range above, where the composition of cosmic rays is still poorly understood.¹³ Furthermore, TAIGA will allow measurements of cosmic ray anisotropies beyond 100 TeV primary energy. Finally, observations of EAS can

also address fundamental questions of particle physics such as measurements of the proton-proton cross-section, or the search for quark-gluon plasma.

2. The TAIGA Experiment

In the TAIGA experiment, a hybrid approach using different detection techniques is used. While both Cherenkov photon and particle identification are used, the term hybrid also, and foremostly, refers to the hybrid Cherenkov technique. The angle-integrating air shower timing array TAIGA-HiSCORE is combined with the imaging air Cherenkov Telescopes TAIGA-IACT. The timing array is a cost effective method for the instrumentation of very large detector areas, and it provides good angular, core position, and energy resolution in the energy range above few 10s of TeV. The IACTs provide the air shower image shape for good gamma-hadron separation. When used in stand alone mode (i.e. no stereo), one IACT can detect air showers at a distance of 300 m - and more - from the shower core. Both detector components together provide the most relevant key parameters: direction and core from HiSCORE-TAIGA and image shape (width, length) from IACT-TAIGA. Placed at a distance of about 600 m from each other, 4 IACTs can cover a HiSCORE array of more than 1 km² area. It has been shown that using such a hybrid approach with only few IACTs per km², combined with a HiSCORE array, achieves a competitive gamma-hadron separation in the energy range above 10 TeV.¹⁴ At energies higher than 100 TeV, the measurement of the muon component of the EAS using particle detectors on the surface and underground will enhance the gamma-hadron separation further.

Currently, TAIGA consists of a total of 120 HiSCORE stations deployed on an area of 1 km², and two 4 m class imaging air Cherenkov telescopes (IACTs) with a 10° aperture. A third IACT is planned for 2022. The distance between the IACTs was chosen as 300 m in the prototype phase of TAIGA. In future, distances of up to 600 m are planned. Additionally, scintillator stations for charged particle detection with a total surface of 240 m² are deployed above and below ground for the measurement of the muon component of EAS. The layout of the TAIGA-HiSCORE and TAIGA-IACT components is shown in Figure 1. The current TAIGA pilot array is used for a proof of principle of the detector concept. In future, an optimized array layout will take advantage of the hybrid method, that allows larger separations between the individual IACTs.

2.1. TAIGA-HiSCORE

HiSCORE is an array of angle-integrating air Cherenkov detector stations, distributed over an area of approximately 1 km². As shown in Figure 1, the stations are arranged in rows offset to each other with inter-station distances of 75 m to 150 m. Each station consists of 4 8 inch (and 10 inch) photomultiplier tubes (PMTs, ElectronTubes and Hamamatsu) with a segmented Winston cone (Alanod 4300UP foil), resulting in a light sensitive area of 0.5 m² per station. The viewing cone of

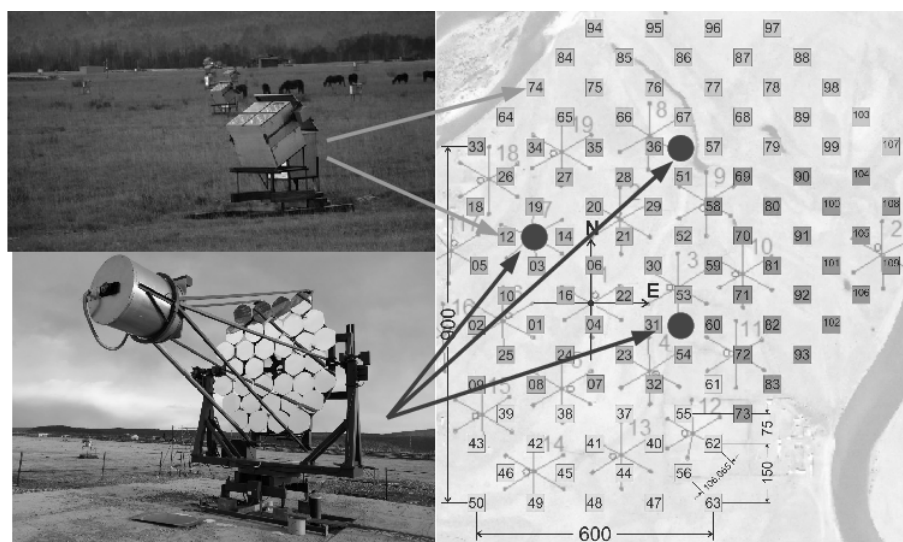


Fig. 1. Layout of the TAIGA-HiSCORE array. Only the HiSCORE and IACT components are shown. The first two IACTs were deployed from 2016 to 2019. The third IACT will be deployed until 2022. The HiSCORE array currently consists of 89 stations and will be extended to 120 stations by the end of 2021.

one station has a diameter of 60° , resulting in an effective field of view of 0.6 sr. An analog summator sums up the signals of all four channels. The sum is used for triggering, and the individual channels are read out with a DRS 4-based 9-channel read-out board at a sampling rate of 2 GHz. Four anode signals and four dynode signals (low gain channel) are read out. Channel number 9 is used for time synchronization, based on the sampling of a 100 MHz clock signal. This custom time-synchronization was cross checked with the WhiteRabbit system. It could be verified that the time synchronization works on a level of 0.2 ns relative timing accuracy.^{15,16} Each detector station is connected to the central DAQ via optical fibre. The signal traces are processed to extract the amplitude and the timing (half-rise-time, full width half maximum). Based on these parameters, the air shower arrival direction, core impact position, and energy are reconstructed using the methods developed for Tunka-133 and HiSCORE.^{1,16,17} Monte Carlo simulations were used to evaluate the detector performance, resulting in resolutions for core position ($O(15\text{m})$), energy (20%), and direction (0.1°). Moreover, the serendipitous discovery of a pulsed signal from the CATS lidar onboard the international space station allowed to verify the absolute pointing of the experiment.

2.2. TAIGA-IACT

Currently, two IACTs are in operation on the TAIGA site. A third IACT is under construction. The TAIGA IACTs are based on a Davies-Cotton design, with

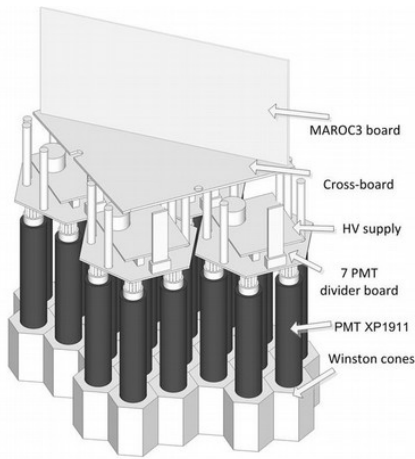


Fig. 2. Layout of a camera cluster of 28 PMTs. The high voltage is supplied to sub-groups of 7 pixels. Each cluster is equipped with a MAROC-3 ASIC board.

a tessellated mirror dish of 34 facets with 60 cm diameter each, resulting in a mirror area of about 10 m^2 . Each axis of the alt-az dish mount mechanics is driven by a stepper motor equipped with shaft-encoders for pointing positioning. Additionally, a sky-CCD system is used for pointing calibration. A verification of the absolute pointing accuracy of 0.02° , was carried out by the measurement of the anode current in the central camera PMT-pixel in a drift-scan across a known bright star position.¹⁸ The PMT camera of IACT-1 consists of 560 XP1911 PMTs (diameter 19mm). The second IACT is equipped with 595 PMTs. Both cameras have a field of view of 9.6° and are placed at the focal point at 4.75 m distance from the respective dishes. For enhanced light collection, and noise suppression from stray light, a Winston Cone plate is attached to the PMT camera plane. The PMTs are organized in clusters of 28 pixels (see Figure 2). All channels are read out with a 64 channel ASIC MAROC-3 board. The board provides a fast shaper which is used for triggering and a slow shaper which is used for read out. The camera electronics for the first two TAIGA-IACT cameras are described elsewhere.^{19, 20}

Air shower event images, such as shown in Figure 3, are reconstructed using the pixel amplitude distributions in the camera, either based on classical moment analysis,²¹ or more advanced machine learning algorithms.²²

2.3. TAIGA Muon array

The TAIGA-Muon array²³ consists of scintillation counters on a total area of currently 240 m^2 . The muon detector stations are distributed above and below ground. In a future stage, a 5 times larger instrumented area is planned. Each TAIGA muon detector consists of four triangular sectors of scintillator material. The sectors are connected with wavelength shifting bars that guide the light to small PMTs (FEU-85). Measurements of cosmic rays have yielded an average cosmic ray muon amplitude of $31\text{p.e.} \pm 20\%$. The TAIGA-Muon array develops its power

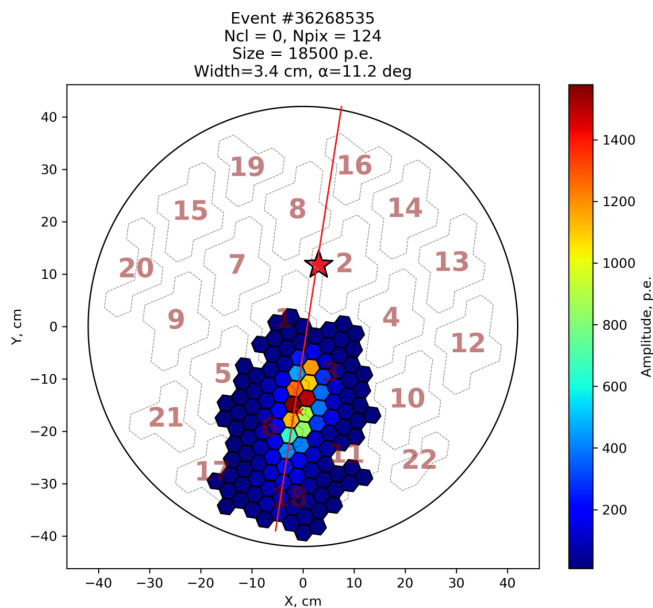


Fig. 3. Real data event for IACT1. The numbered shapes correspond to the above described clusters. The star shows the direction of the air shower event as reconstructed by the HiSCORE array. The total amplitude summed over pixels (size) is 18500 photoelectrons (p.e.). The alpha angle of the major axis is 11.2 degrees, and the measured image with (second image moment) is 0.41 degrees.

at higher energies, starting at about 100 TeV, where the measurement of the muon component of EAS helps in discriminating hadrons from gamma-rays, as well as identifying the nature of the hadronic cosmic rays.

2.4. Hybrid technique

A large instrumented detector area is key for accessing very high energies from few TeV to several 100s of TeV. Using only IACTs and the well-established stereoscopic technique requires a large number of channels per instrumented km^2 , because firstly, each IACT has a large number of camera channels, and secondly, the IACTs cannot be placed too far away from each other, in order to detect the same EAS in at least two IACTs for stereoscopic reconstruction. As opposed to that, the instrumentation of large areas with a timing array such as HiSCORE is more cost effective, requiring considerably lower number of channels per km^2 . However, while gamma-hadron separation is possible with HiSCORE alone to a certain degree (and improving with increasing energy¹⁷), the separation power stays below the quality reached with IACTs. Therefore, TAIGA implements a novel hybrid technique, taking advantage of the strengths of both Cherenkov techniques. The effective area is maximized using the timing array principle, and the gamma-hadron separation is optimized using

the IACTs. More specifically, the strong points of HiSCORE are the directional and core position resolution. The strength of the IACTs is the image shape. The IACTs can be placed so far apart from each other, that each IACT is operated in monoscopic mode, meaning that the Cherenkov lightpool of one air shower event only hits one IACT, as shown in Figure 4. Without requiring a stereoscopic trigger, the effective area of each IACT can be fully exploited and only 4 IACTs are needed in order to cover an area of the order of 1 km^2 . The loss of reconstruction quality when using the IACTs in monoscopic mode as compared to stereoscopic mode can be recuperated using the information of the HiSCORE array on angular and core position, as illustrated in Figure 5. The major axis of the IACT image in that Figure is pointing towards the core position, which cannot be reconstructed with the IACT alone, but is provided by the HiSCORE array. For comparison, a classical method for hadron suppression in stereoscopic systems is to use the mean scaled width parameter, for which the core position is reconstructed stereoscopically and the image widths of all IACTs are scaled according to MC-expectation. A similar parameter in TAIGA is the hybrid scaled width, which is the image width from one IACT, scaled with the MC-expectation for the given image size and using the core position and direction as reconstructed by HiSCORE. It was shown that the hybrid scaled width achieves competitive rejection power.¹⁴ As opposed to stereoscopic systems, this method does not suffer from deteriorating core impact resolution at large distances (over the full HiSCORE array, the core resolution is the same) and also does not require closely spaced IACTs. The sensitivity of the air Cherenkov components of the TAIGA experiment was estimated using MC-simulations and is shown in Figure 6.

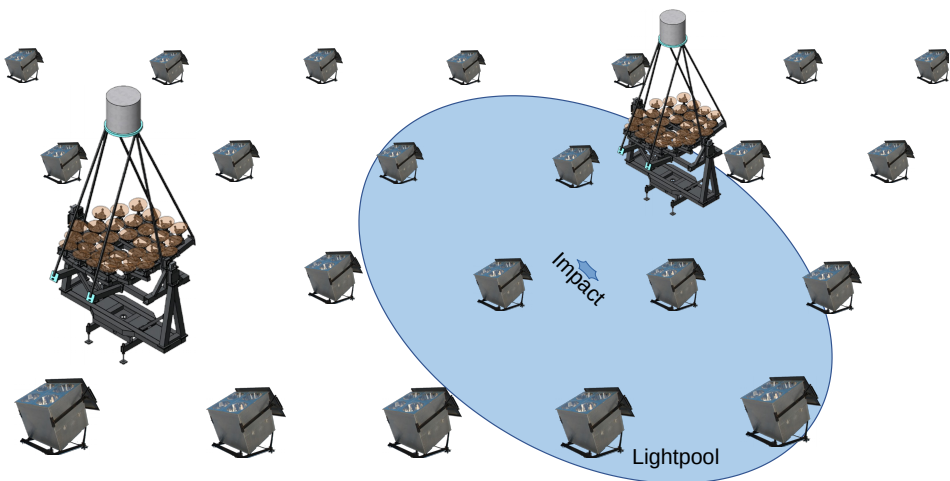


Fig. 4. Schematical drawing of the principle of hybrid operation.

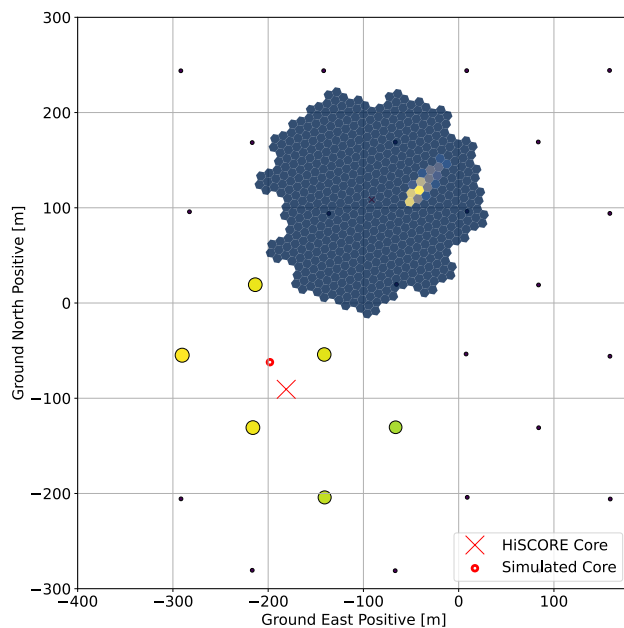


Fig. 5. Simulated hybrid event: as explained in Figure 4, the EAS impact position is reconstructed using the HiSCORE array. The major IACT image axis projected to the ground reference frame (not drawn) is pointing towards the position of the reconstructed core impact position.

3. First results

3.1. TAIGA-HiSCORE

The angle integrating HiSCORE array was installed in several stages since 2016. The performance of the array was estimated using from MC-simulations and real data. The relative angular and core position resolutions using a subdivision of the array into subarrays (chessboard method) could be reproduced in simulations, verifying the expected performance of TAIGA-HiSCORE.²⁴ The relative station timing is calibrated using stationary light sources and air shower data. A fast moving source in the field of view of the array turned out to be the CATS Lidar onboard the international space station. This light source could be used to verify time synchronization and absolute array pointing.^{15,16} As compared to the Tunka-133 array, the measurement of the cosmic ray energy spectrum could be extended to lower energies with TAIGA-HiSCORE, as indicated in Figure 7.

3.2. TAIGA-IACT

The MC detector simulation for the TAIGA-IACTs is done using two simulation chains: a custom MC simulation chain, and an adaptation of the *sim_telarray* package.²⁵ The image pixel photoelectron scale is calibrated using an LED illuminating

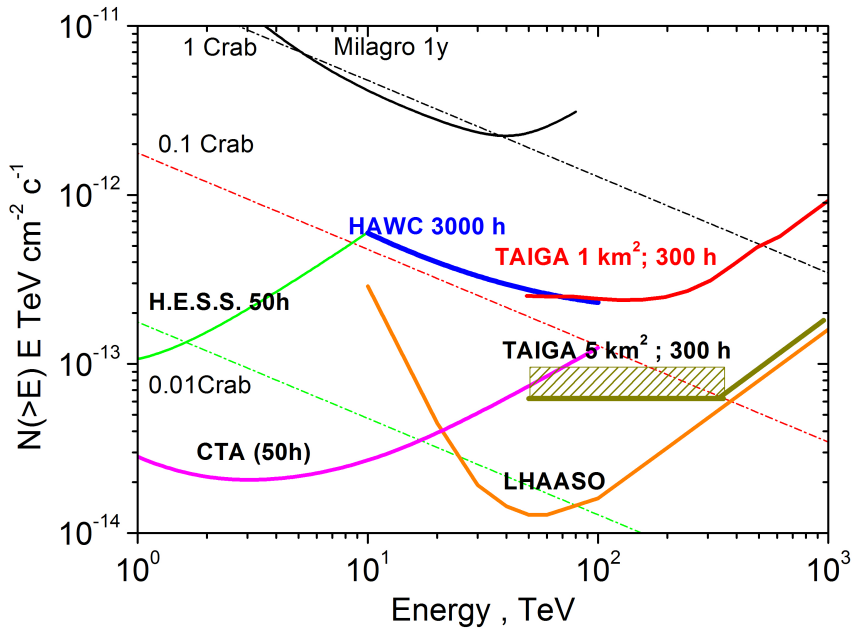


Fig. 6. Sensitivity of the TAIGA experiment for 300 hours of observations in hybrid mode (without moon detectors). A comparison to sensitivities of other experiments is not straight forward, since also the angular and spectroscopic resolutions play an important role for measurements of the morphology and spectra of astrophysical objects. TAIGA has a relative energy resolution of better than 20% and an angular resolution of the order of 0.1° .

the whole PMT camera. Raw data are processed using two independent reconstruction chains to obtain air shower images (amplitude distributions of all pixels for each event). Four different high-level analyses, based on the robust Hillas-parameters, were applied to these image data. Figure 8 shows a comparison of the amplitude distributions of the second-hottest pixel in real data and simulation. A comparison of simulated and real image width is shown in Figure 9. The simulations describe real data reasonably well.

After commissioning of the first TAIGA-IACT, our primary goal was to demonstrate that the IACT is operational. For this purpose, observations of the standard candle, the Crab Nebula, were carried out. After weather quality selection, a total data set of 40.5 h is obtained for analysis. Observations were taken in the wobble mode (Wobble offset 1.2°). The position of the Crab Nebula inside the IACT camera is taken as the on-source region and the background was estimated from off-source regions at identical distances to the camera center, from the same dataset. The distribution of the alpha angle between the major image axis and the position of the Crab Nebula inside the camera is shown in Figure 10. Selecting events with an image size of at least 120 p.e., a clear excess can be observed. With a zenith angle of 31° , and taking into account the altitude of the observation level, the efficiency

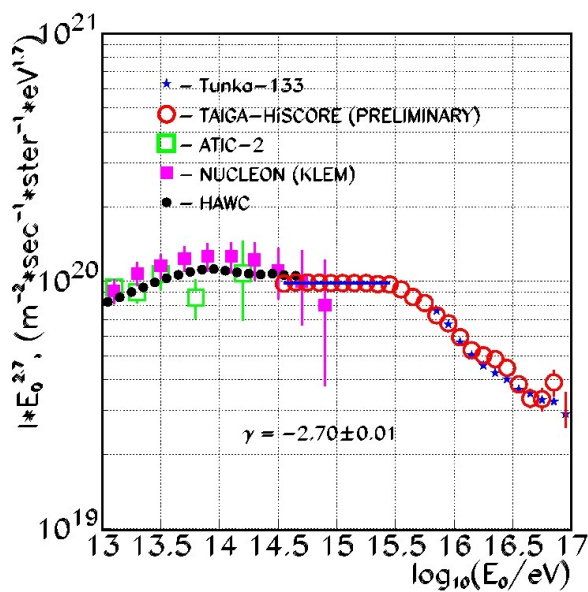


Fig. 7. The all-particle cosmic ray spectrum measured with TAIGA-HiSCORE, compared to different measurements by other experiments.

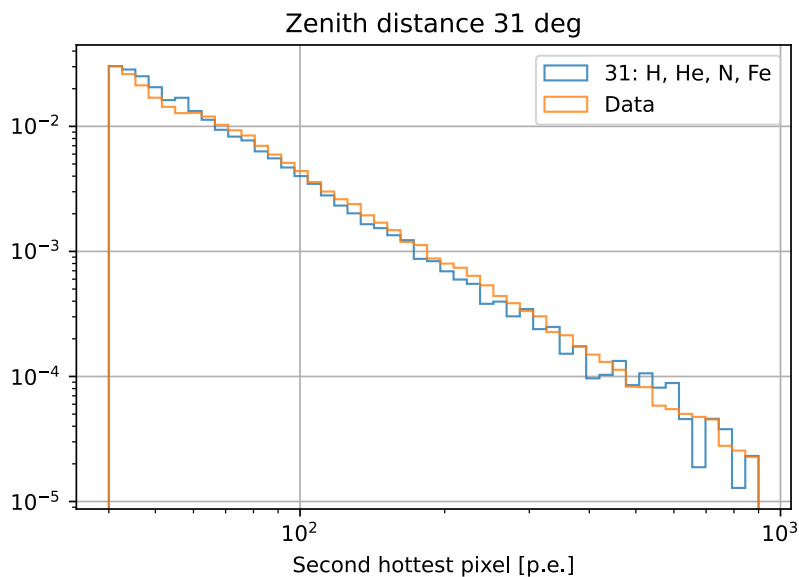


Fig. 8. Distribution of the amplitude of the second-hottest pixel in IACT-1. Data are shown in light grey, simulations are shown in dark grey.

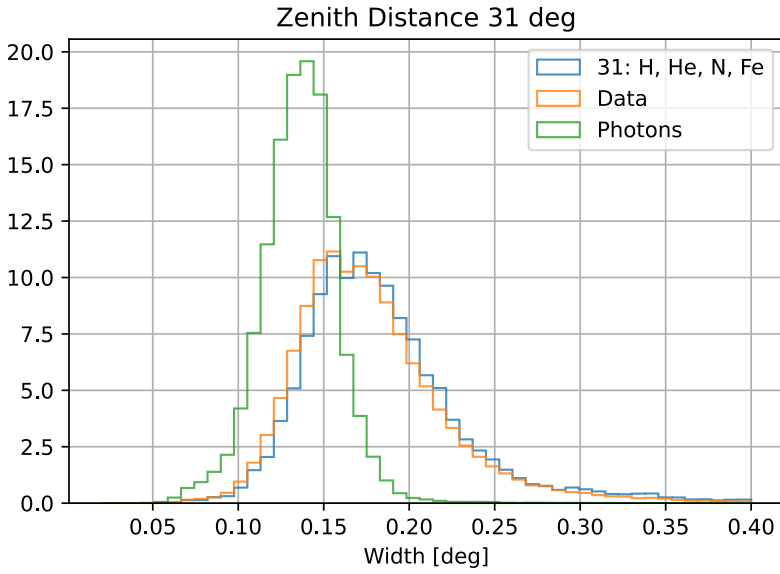


Fig. 9. Distribution of the image width for MC and real data.

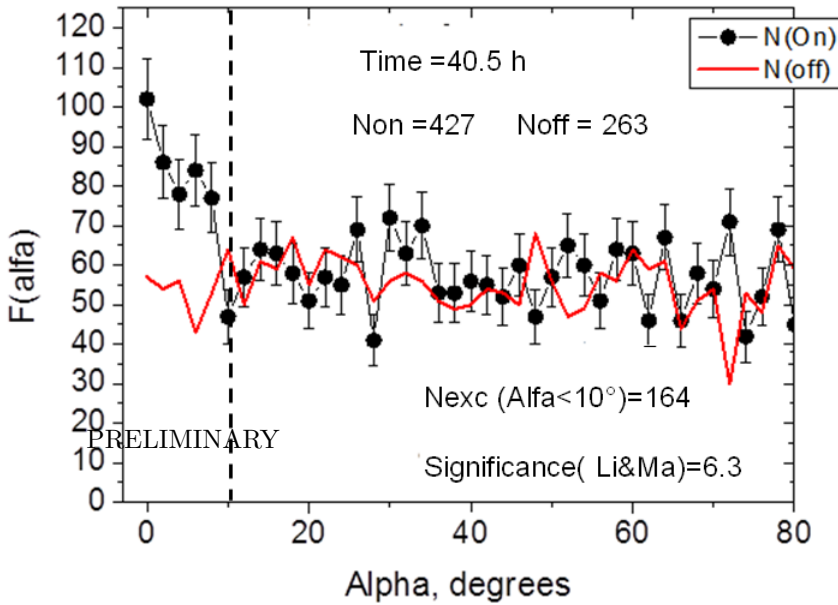


Fig. 10. Distribution of the alpha angle for all runs of a dataset of 42 hours from the Crab Nebula. These preliminary results are currently being finalized to be included in an upcoming journal publication.

of the optical system, and the cuts applied, the energy threshold of this data set is 4.5 TeV. The significance²⁶ of the observed excess is 6.3σ (using a cut on alpha smaller than 10deg).

4. Conclusion

The novel hybrid technique of the TAIGA pilot array combines the angle integrating air Cherenkov timing technique with 4 m class imaging air Cherenkov telescopes, taking advantage of the strengths of both techniques, i.e. large instrumented areas with the HiSCORE array, and gamma-hadron separation from image shape using the IACTs. Additionally, a scintillator detector for particle detection above and below ground will allow the measurement of the muon component, for improved gamma-hadron separation at higher energies. The expected sensitivity of the future 5 km² stage is in the region of 10^{-13} photons cm⁻²s⁻¹. First stages of the 3 TAIGA detector components are in operation. Monte Carlo simulations were compared to real data, showing a good understanding of the detectors. Observations of the Crab Nebula for 40.5 h above 4.5 TeV resulted in an excess of 6.3σ .

Acknowledgments

The work was performed at the UNU “Astrophysical Complex of MSU-ISU” (agreement 13.UNU.21.0007). The work is supported by Russian Foundation for Basic Research (grants 19-52-44002, 19-32-60003), the Russian Science Foundation (grant 19-72-20067 (Section D,E), the Russian Federation Ministry of Science and High Education (projects FZZE-2020-0017, FZZE-2020-0024), by the Deutsche Forschungsgemeinschaft (DFG, TL 51/6-1) and by the Helmholtz Association (HRJRG-303) and by European Union’s Horizon 2020 programme (No. 653477). D.H., M.T, A.K.A. and M.B. acknowledge support by the Deutsche Forschungsgemeinschaft (DFG, German Research Foundation) under Germany’s Excellence Strategy — EXC 2121 “Quantum Universe” — 390833306.

References

1. S. F. Berezhnev, D. Besson, N. M. Budnev, A. Chiavassa, O. A. Chvalaev, O. A. Gress, A. N. Dyachok, S. N. Epimakhov, A. Haungs, N. I. Karpov, N. N. Kalmykov, E. N. Konstantinov, A. V. Korobchenko, E. E. Korosteleva, V. A. Kozhin, L. A. Kuzmichev, T. Collab.) *et al.*, *Nucl. Instrum. Methods* **692**, p. 98 (2012).
2. S. D. Hunter, D. L. Bertsch, J. R. Catelli, T. M. Dame, S. W. Digel, B. L. Dingus, J. A. Esposito, C. E. Fichtel, R. C. Hartman, G. Kanbach, D. A. Kniffen, Y. C. Lin, H. A. Mayer-Hasselwander, P. F. Michelson, C. von Montigny, R. Mukherjee, P. L. Nolan, E. Schneid, P. Sreekumar, P. Thaddeus and D. J. Thompson, *The Astrophysical Journal* **481**, 205 (May 1997).
3. A. A. Abdo, B. Allen, D. Berley, E. Blaufuss, S. Casanova, C. Chen, D. G. Coyne, R. S. Delay, B. L. Dingus, R. W. Ellsworth and et al., *The Astrophysical Journal* **658**, p. L33–L36 (Feb 2007).

4. F. Aharonian, A. G. Akhperjanian, A. R. Bazer-Bachi, B. Behera, M. Beilicke, W. Benbow, D. Berge, K. Bernlöhr, C. Boisson, O. Bolz and et al., *Astronomy & Astrophysics* **481**, p. 401–410 (Jan 2008).
5. A. Abramowski, F. Aharonian, F. A. Benkhali *et al.*, *Nature* **531**, p. 476–479 (Mar 2016).
6. S. Gabici and F. A. Aharonian, *The Astrophysical Journal* **665**, p. L131–L134 (Aug 2007).
7. T. Glauch, in *Proceedings of the 3rd International Symposium on Cosmic Rays and Astrophysics (ISCRA-2021), 8–10 June 2021*.
8. Z. Cao, F. Aharonian, Q. An *et al.*, *Nature* **594**, p. 33–36 (2021).
9. T. Kneiske and D. Horns, in *38th COSPAR Scientific Assembly*,
10. I. V. Moskalenko, T. A. Porter and A. W. Strong, *Astr. Phys. J. L.* **640**, L155 (April 2006).
11. F. D. Steffen, *European Physical Journal C* **59**, 557 (January 2009).
12. H.-S. Zechlin, D. Horns and J. Redondo, in *American Institute of Physics Conference Series (2008)*, eds. F. A. Aharonian, W. Hofmann and F. Rieger.
13. L. Anchordoqui, M. T. Dova, A. Mariazzi, T. McCauley, T. Paul, S. Reucroft and J. Swain, *Ann. Phys. (N.Y.)* **314**, p. 145 (2004), hep-ph/0407020.
14. M. Kunas, PhD thesis, University of Hamburg (2017), <https://ediss.sub.uni-hamburg.de/handle/ediss/7582>.
15. O. Gress, I. Astapov, N. Budnev, P. Bezyazeev, A. Bogdanov, V. Boreyko, M. Brückner, A. Chiavassa, O. Chvalaev, A. Dyachok, T. Gress, S. Epimakhov, E. Fedoseev, A. Gafarov, N. Gorbunov, V. Grebenyuk, (TAIGA Collab.) *et al.*, *Nucl. Instrum. Methods A* **845**, p. 367 (2017).
16. A. Porelli, D. Bogorodskii, M. Brückner, N. Budnev, O. Chvalaev, A. Dyachok, S. Epimakhov, T. Eremin, O. Gress, T. Gress, D. Horns, A. Ivanova, S. Kiruhin, E. Konstantinov, E. Korosteleva, M. Kunas *et al.*, *J. Phys.: Conf. Ser.* **632**, p. 012041 (2015).
17. D. Hampf, M. Tluczykont and D. Horns, *Nucl. Instrum. Methods A* **712**, p. 137 (2013).
18. D. Zhurov, in *Proceedings of the 36th International Cosmic Ray Conference (ICRC2019)*.
19. N. Lubsandorzhev, I. Astapov, P. Bezyazeev, V. Boreyko, A. Borodin, M. Brueckner, N. Budnev, A. Chiavassa, A. Dyachok, O. Fedorov, A. Gafarov, A. Garmash, N. Gorbunov, V. Grebenyuk, O. Gress, T. Gress, (TAIGA collab.) *et al.*, in *Proceedings of the 35th International Cosmic Ray Conference (ICRC2017)*.
20. N. Lubsandorzhev, in *Proceedings of the 36th International Cosmic Ray Conference (ICRC2019)*.
21. A. M. Hillas, in *Proceedings of the 19th International Cosmic Ray Conference (1985)*.
22. R. Parsons and S. Ohm, *Eur. Phys. J. C* **80**, p. 363 (2020).
23. I. I. Yashin, I. I. Astapov, N. S. Barbashina, A. G. Bogdanov, V. Boreyko, N. M. Budnev, M. Büker, M. Bruckner, A. Chiavassa, O. B. Chvalaev, A. V. Gafarov, N. Gorbunov, V. Grebenyuk, O. A. Gress, A. Grinyuk, O. G. Grishin, (TAIGA collab.) *et al.*, *J. Phys.: Conf. Ser.* **675**, p. 032037 (2016).
24. M. Tluczykont, O. Gress, E. Korosteleva, L. Kuzmichev, A. Pakhorukov, A. Porelli, V. Prosin, L. Sveshnikova, R. Wischnewski, I. Astapov, P. Bezyazeev, V. Boreyko, A. Borodin, M. Brueckner, N. Budnev, A. Chiavassa, (TAIGA Collab.) *et al.*, in *Proceedings of the 35th International Cosmic Ray Conference (ICRC2017)*.
25. K. Bernlöhr, *Astropart. Phys.* **30**, p. 149 (2008).
26. T. Li and Y. Ma, *Astrophys. J.* **272**, p. 317 (1983).